The final publication is available at

https://doi.org/10.1016/j.cattod.2017.10.034

Additional Information

Type I *vs* Type II Photodegradation of Pollutants

R. Martinez-Haya,[a] M.A. Miranda[a,*] and M. L. Marin[a,*]

[a]Instituto de Tecnología Química, Universitat Politècnica de València-Consejo Superior de Investigaciones Científicas, Avda. de los Naranjos s/n, E-46022, Valencia, Spain

*Corresponding author

E-mail addresses: mmiranda@qim.upv.es; marmarin@qim.upv.es

Abstract

Rose Bengal (RB) is a widely used photocatalyst due to its high quantum yield of singlet oxygen ($^1O_2$) formation. Hence, when RB has been employed for wastewater remediation, the observed photodegradation has been attributed to reaction between the pollutants and the $^1O_2$ formed (Type II mechanism). However, RB could also react, in principle, via electron transfer (Type I mechanism). Herein, competition between Type I vs Type II oxidation has been investigated for RB in the photodegradation of emerging pollutants such as diclofenac (DCF) and acetaminophen (ACP). In parallel, the photocatalyst perinaphthenone (PN) has also been evaluated for comparison. The degree of removal achieved for both pollutants in aerated/deaerated aqueous solutions irrespective of the employed photocatalyst does not support the involvement of $^1O_2$ as the main species responsible for removal of the pollutants. Photophysical experiments showed that the triplet excited states of RB and PN are efficiently quenched by both DCF and ACP. Moreover, $^1O_2$ emission was also quenched by DCF and ACP. Thus the contribution of Type I versus Type II in the photodegradation has been evaluated from the experimentally determined rate constants. Nevertheless, at the upper limit for the typical concentration of emerging pollutants (10^{-5} M) photodegradation proceeds mainly via Type I mechanism.

1. Introduction

Rose Bengal (RB) (Figure 1) is a well-known photocatalyst that has been widely used due to its high quantum yield of singlet oxygen ($^1O_2$) formation ($\Phi_\Delta = 0.76$-0.83).[1-5] For this reason, when it has been employed for wastewater remediation for the study of photochemical behavior of natural waters, the observed photodegradation has been, in general, attributed to reaction between the pollutants and the $^1O_2$ formed (Type II mechanism).[6-9] However, RB with a redox potential of $E_{RB/RB^{\cdot-}} = -0.95$ V vs SCE, could also react, in principle, via electron transfer (Type I mechanism).[10-12] In the context of water remediation, Type I reactions would be more favored than Type II, due to: i) the higher relative permittivity value of water compared to polar organic solvents, such as acetonitrile, ($\varepsilon_{H2O} = 80.16$ vs $\varepsilon_{ACN} = 35.94$); ii) the lower concentration of O_2 (0.29 mM in water vs 1.9 mM in acetonitrile); and iii) the lower lifetime of $^1O_2$ (2 μs in water vs 68 μs in acetonitrile).[13, 14] Furthermore, RB has a high Φ_{ISC} (Figure 1), and Type I photodegradation processes happen mainly from the triplet excited states, due to the longer lifetime of the triplets compared to that of the singlets.[15] Therefore, competition between Type I vs Type II oxidation deserves further investigation to establish the real mechanism involved in the photodegradation processes that often take place in aqueous solutions.

Herein, RB has been employed to investigate the photodegradation of two representative commonly used drugs, such as diclofenac (DCF) and acetaminophen (ACP) found in real wastewaters at low concentrations (see Figure 2). For a deeper understanding of the Type I/Type II competition, a second photocatalyst, perinaphtenone (PN), less widely employed but with a higher $^1O_2$ quantum yield formation (Φ_Δ ca 1) and a $E_{PN/PN^{\cdot-}} = -0.62$ V vs SCE, has also been evaluated using the same representative pollutants.[16, 17] Laser flash photolysis and transient emission spectroscopy experiments of RB/PN in the presence of the contaminants provided valuable fast-kinetic data. From the determined quenching rate constants, the

4

contribution of Type I/Type II mechanisms in the photodegradation of the selected contaminants has been evaluated and a general conclusion has been drawn.

Perinaphthenone (**PN**)

Rose Bengal (**RB**)
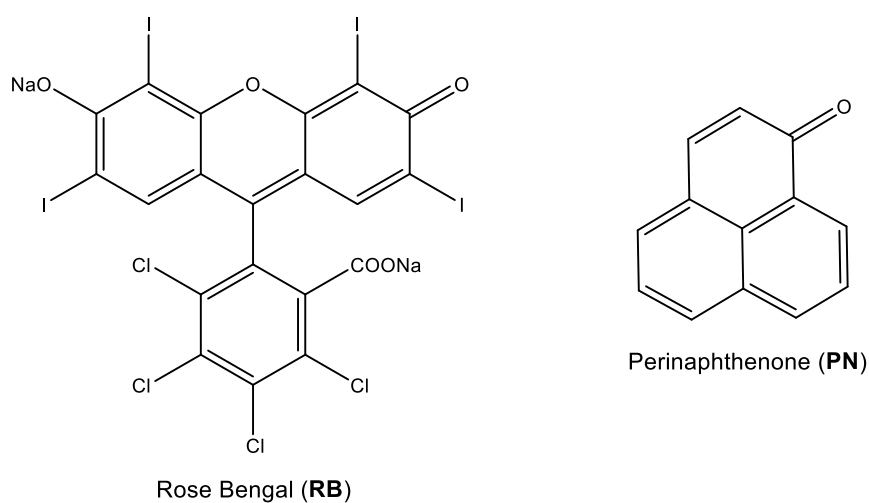
Data	**RB**[12]	**PN**[17]
Φ_{isc}	0.77	1
E_T (eV)	1.8	1.9
E_{red} (PC/PC$^{\bullet -}$) (V vs SCE)	-0.95	-0.62

Fig. 1. Chemical structures, photophysical properties such as intersystem crossing quantum yield (Φ_{isc}) or energy of the triplet excited state (E_T) together with electrochemical details, such as redox potentials (E_{red} (PC/PC$^{\bullet -}$) of the selected photocatalysts.

Diclofenac (**DCF**)   Acetaminophen (**ACP**)
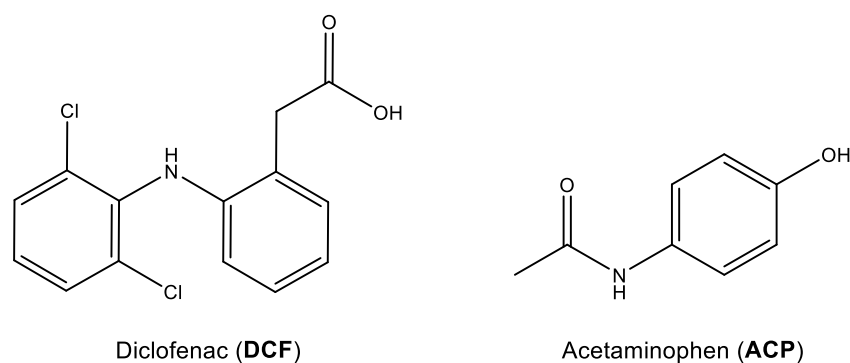
Fig. 2. Chemical structures of the selected contaminants.

2. Experimental

2.1. Reagents

Diclofenac (DCF), acetaminophen (ACP), 4-nitrobenzoic acid, Rose Bengal disodium salt (RB) and perinaphthenone (PN) were obtained from Aldrich. Water was Milli-Q grade and acetonitrile (ACN) was of HPLC quality from Scharlau.

2.2. Photochemistry

Photochemical reactions were performed in Pyrex glass tubes with magnetic stirring. For the reactions photocatalyzed by RB, a home-made photoreactor built with a spiral set-up of 2.5 m strip green LEDs (λ_{em} centered at 515 nm), Samsung SMD5630IP20 of 40 W was employed; whereas for the reactions photocatalyzed by PN, a Luzchem photoreactor (model LZC-4 V) with 14 bulbs emitting at 420 nm was used. Aqueous solutions (16 mL) containing a mixture of the two pollutants (5×10^{-5} M each) and either RB or PN (10 mg L^{-1}) were irradiated under air or N$_2$ atmosphere. To monitor the removal of the pollutants, aliquots of 90 μL were taken at different irradiation times, and were analyzed by HPLC, using 4-nitrobenzoic acid (10 μL of a 0.1 mM solution) as internal standard. The equipment was an Agilent 1220 Infinity LC model with a quaternary pump G4290B, photodiode detector G4290B and wavelength detection from 200 to 360 nm equipped with a Mediterranea Sea 18 column (25 cm $\times$ 0.46 cm, 5 μm particle size). The mobile phase was a gradient mixture of water (pH 3):ACN (70:30-30:70) at a flow rate of 1.5 mL min^{-1}; the detection wavelength was fixed at 250 nm.

2.3. Photophysical instrumentation

Absorption spectra (UV/Vis) were recorded on a Cary 50 (Varian) spectrophotometer. A pulsed Nd: YAG SL404G-10 Spectron Laser Systems at the excitation wavelength of 355 nm or 532 nm in the case of PN or RB, respectively, was employed to carry out the laser flash photolysis (LFP) experiments. The energy of the single pulses (~10 ns duration) was lower than 30 mJ pulse^{-1}. The laser flash photolysis system is formed by the pulsed laser, a pulsed Lo255 Oriel Xenon lamp, a 77200 Oriel monochromator, an Oriel photomultiplier tube (PMT) housing, a

70705 PMT power supply and a TDS-640A Tektronix oscilloscope. Lifetime of singlet oxygen was recorded at 1270 nm with a Hamamatsu NIR detector (peltier cooled at -62.8º C operating at 800 V, coupled to a grating monochromator) upon excitation with a 355 nm Nd:YAG laser. A customized Luzchem Research LFP-111 system was employed to collect and process the data.

2.4. Photophysical experiments

Quartz cells of 1 cm optical path length were employed for all photophysical measurements, which were run at room temperature. For the laser flash photolysis experiments, increasing amounts of pollutants (up to 3 mM) were added to ACN:H_2O (4:1) solutions of RB or PN (absorbance *ca.* 0.3 at 355 or 532 nm for PN or RB, respectively), under N_2 atmosphere. Lifetime of singlet oxygen was determined from phosphorescence decay curves at 1270 nm upon increasing amounts of pollutant (up to 3 mM) in aerobic ACN:H_2O (4:1) solutions.

2.5. Electrochemical measurements

Electrochemical measurements were carried out using a computer-controlled potentiostat Autolab PGSTAT302N Metrohm. A three-electrode electrochemical cell was employed for the electrochemical measurements. The working, counter, and pseudo-reference electrodes were glassy carbon, Pt-wire and Ag-wire electrodes, respectively. The potentials were measured with respect to ferrocene couple (Fc^+/Fc) at room temperature in an Eppendorf cup degassed with Ar using tetrabutylammonium tetrafluoroborate 0.1 M from Fluka. Scan rate: 0.2 V/s.

3. Results and discussion

3.1. Photodegradation

Degradation of the pollutants photocatalyzed by RB was evaluated in aqueous aerobic and anaerobic media, upon selective excitation of the photocatalyst. Fig. 3 top shows the results obtained up to 9.5 hours; removal of DCF was easily achieved, however ACP was not

completely degraded (*ca.* 50% and 40% in aerobic and anaerobic media respectively). Parallel irradiation experiments were carried out using PN in aqueous aerobic and anaerobic media (Fig. 3 bottom). The degree of removal achieved for both pollutants was indeed higher when using PN than RB as photocatalyst. Although one can expect a better performance of the photodegradation when PN is used as photocatalyst considering that the $^1O_2$ quantum yield of PN is higher than the $^1O_2$ of RB, this assumption is not in agreement to the experimental results; since the photodegradation takes place at the same extent under anaerobic media, regardless the photocatalyst used. Therefore, these results obtained in aerated/deaerated aqueous media do not support the involvement of $^1O_2$ as the main species responsible for the removal of the pollutants. Hence, Type II appears to be inefficient in the aerobic photodegradation.[18]

Control experiments in the absence of photocatalyst but upon irradiation or in the presence of the photocatalyst but in the absence of light were carried out. Only direct photolysis of DCF produced *ca* 20% of degradation after 6 hours of irradiation.
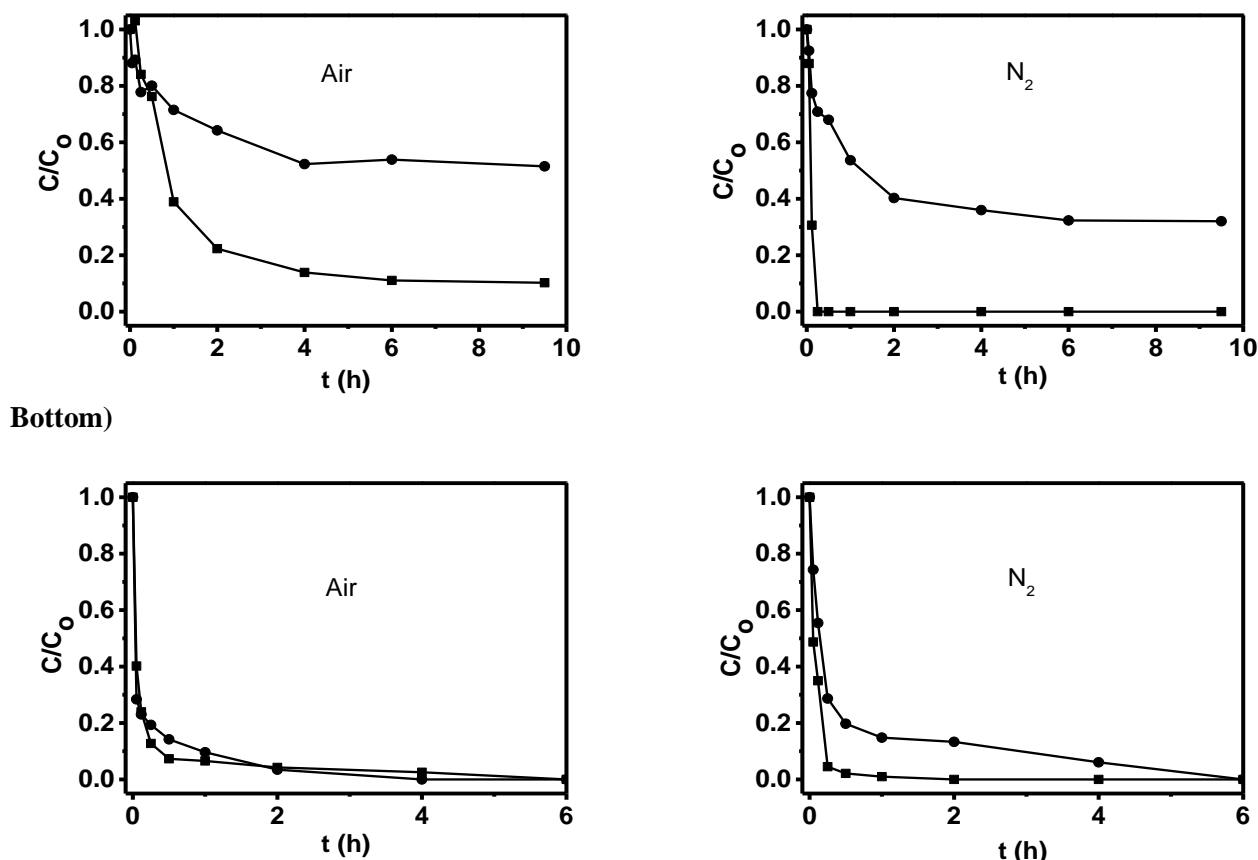
Top)

Fig. 3. Plot of the relative concentration of DCF (■) and ACP (●), $C_o = 5 \times 10^{-5}$ M each, *vs.* irradiation time, in the presence of 10 mg L^{-1} of RB (top) or PN (bottom), in aqueous solution and different atmospheres. Graphs on the left show the relative concentration evolution of the photocatalytic degradations run under air; whereas graphs on the right show the relative concentration evolution of the photocatalytic degradations run under nitrogen.

3.2. Mechanistic studies

3.2.1. Type I mechanism

Laser flash photolysis experiments were carried out to determine the involvement of the triplet excited state of each photocatalyst in the photodegradations. Type I mechanisms are more sensitive to the polarity of solvents than Type II ones. In fact, polar solvents, such as water, favor Type I mechanisms due to their higher capability to stabilize charged species. However, the photophysical measurements were recorded in the less favorable ACN:H$_2$O (4:1) due to the

9

higher solubility at the concentrations needed. Thus, quenching of the triplet excited state of RB by the contaminants was recorded in ACN:H_2O (4:1) (see Fig. 4 and the kinetic constants were in the order of 10^7 - 10^8 $M^{-1}s^{-1}$ (Fig. 5 and Table 1). Likewise, $^3PN^*$ was efficiently quenched by both pollutants with k_q values in the range of 10^8 $M^{-1}s^{-1}$ (Fig. 4, Fig. 5 and Table 1). The observed quenchings could be due to the electron transfer from the pollutants to the triplet excited states of the photocatalysts. In our hands, the experimentally determined redox potentials were E_{red} ($DCF^{•+}/DCF$) = 0.75 V *vs* SCE and E_{red} ($ACP^{•+}/ACP$) = 1.15 V *vs* SCE. Thermodynamic estimations using these redox potentials indicate that photodegradation *via* Type I mechanism is thermodynamically favored for DCF; whereas for the case of ACP it is exergonic when using PN while slightly endergonic for the case of RB.[19, 20] In agreement with thermodynamic estimations, the spectra recorded after addition of the pollutants showed the expected reduced $PN^{•-}$ (Fig. 6). In addition, both photocatalysts were also efficiently quenched by O_2. For RB, a complete quenching of the triplet excited state happened in the presence of air, thus it was not possible to obtain an accurate value, therefore the diffusion control data was taken for the calculations.[21] In the case of PN, the experimental kinetic constant value was k_q = 2.1 x 10^9 $M^{-1}s^{-1}$.
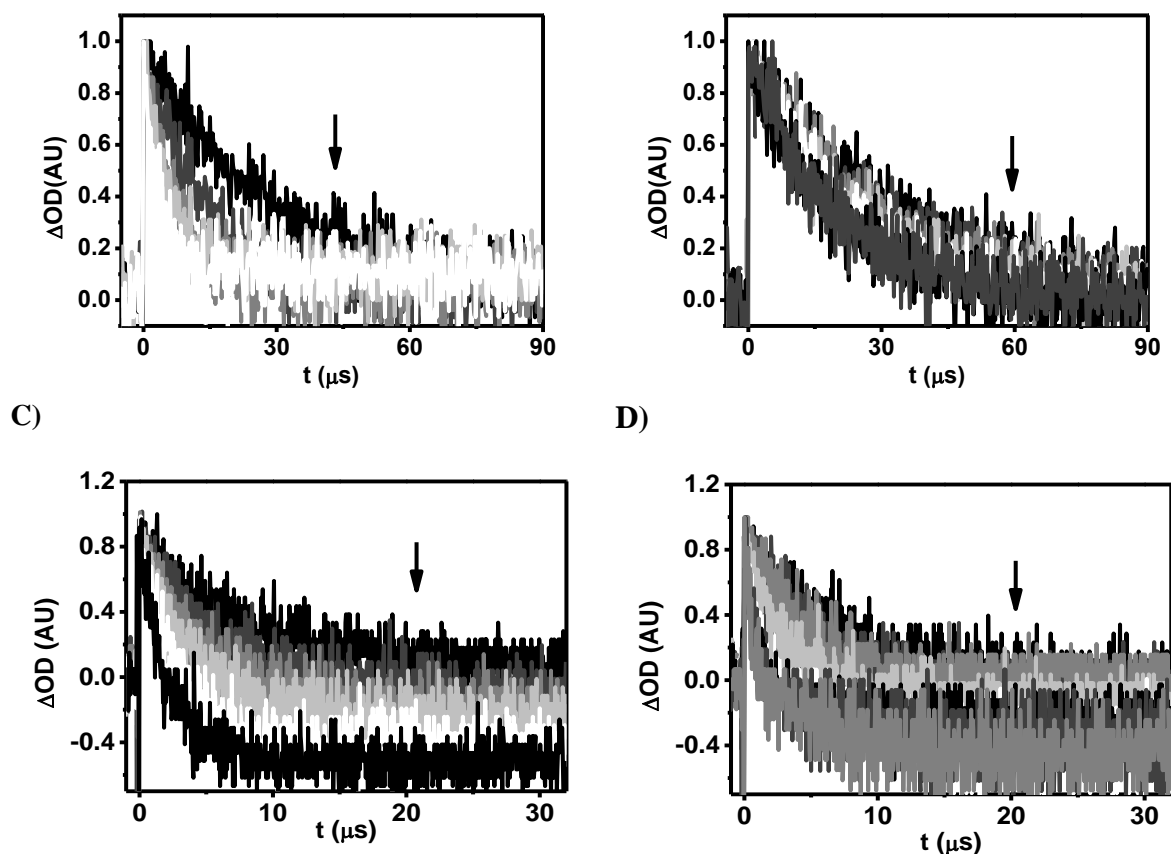
A)   **B)**

Fig. 4. Kinetic traces corresponding to the triplet excited states of $^3RB^*$ (top, recorded at 610 nm) or $^3PN^*$ (bottom, recorded at 390 nm), respectively, in ACN:H_2O (4:1), upon increasing concentrations of ACP (left graphs, **A**, **C**) or DCF (right graphs, **B**, **D**) (A≈0.3 at λ_{exc} = 532 nm or λ_{exc} = 355 nm, for the laser flash photolysis excitation of RB or PN, respectively).
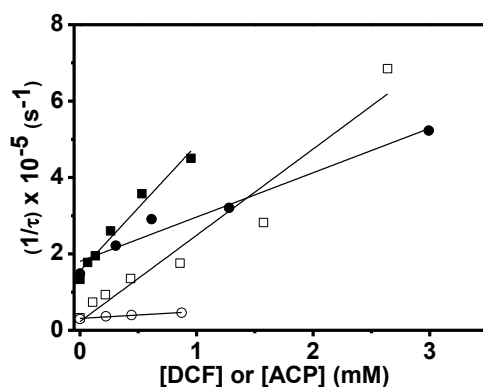

Fig. 5. Stern-Volmer plots obtained for the quenching of $^3RB^*$ (blank symbols) or $^3PN^*$ (solid symbols) by increasing concentrations of ACP (squares) and DCF (circles) in ACN:H_2O (4:1).

Table 1. Quenching rate constants of $^3RB^*$, $^3PN^*$ and $^1O_2$ by the two pollutants. (1) Diffusion control in water.[21]

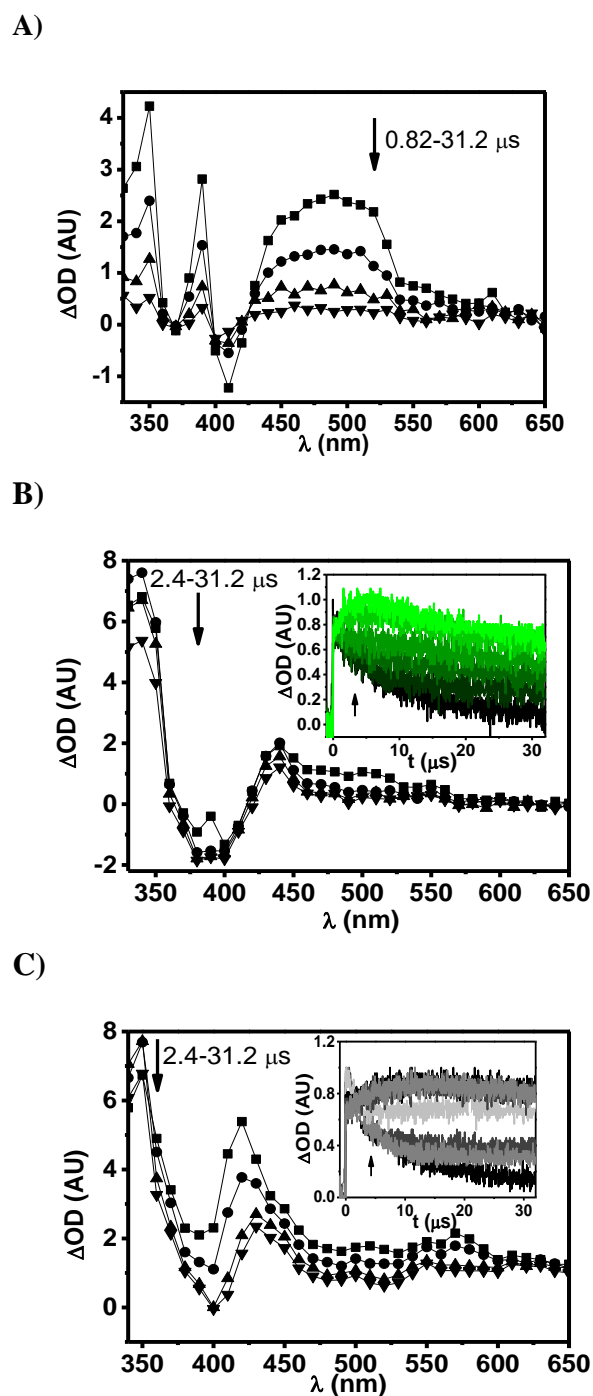|	$^3RB^*$	$^3PN^*$	$^1O_2$
	$k_q\,/\,M^{-1}s^{-1}$	$k_q\,/\,M^{-1}s^{-1}$	$k_q\,/\,M^{-1}s^{-1}$
DCF	$(1.8 \pm 0.3) \times 10^7$	$(1.2 \pm 0.1) \times 10^8$	$(9.7 \pm 1.2) \times 10^6$
ACP	$(2.3 \pm 0.2) \times 10^8$	$(3.3 \pm 0.3) \times 10^8$	$(2.3 \pm 0.2) \times 10^7$
O₂	7.4×10^9 (1)	$(2.1 \pm 0.1) \times 10^9$	-

A)

B)

C)

Fig. 6. Transient absorption spectra of PN obtained at different times after the laser pulse in the absence of the pollutants (**A**) or in the presence of ACP (**B**) or DCF (**C**) (both 1 mM). Insets: Decay traces recorded at 350 nm upon increasing concentrations of ACP (**B**) or DCF (**C**) (both 0 – 1 mM). Laser flash photolysis experiments were performed in deaerated ACN:H_2O (4:1), A_{PN} *ca.* 0.3 at λ_{exc} = 355 nm.

3.2.2. Type II mechanism

The involvement of $^1O_2$ was evaluated by recording its characteristic emission band at 1270 nm, upon increasing concentration of the pollutants. Then, the reverse of the lifetime after each addition was plotted *vs* pollutant concentration and the experimental values were fitted using the Stern-Volmer equation. As it can be seen in Fig. 7, $^1O_2$ was quenched by the pollutants with k_q in the range $10^6 - 10^7$ $M^{-1}s^{-1}$ (Table 1).
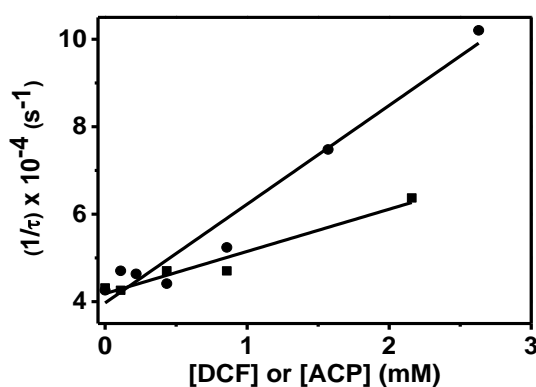

Fig. 7. Stern-Volmer plots for the quenching of the emission due to $^1O_2$ by increasing concentrations of DCF (■) and ACP (●).

3.2.3. Type I versus Type II overall kinetic analysis

Photodegradation of the pollutants by RB and PN can, in principle, happen *via* Type I (electron transfer to the triplet excited state of the photocatalysts) and also *via* Type II (reaction with $^1O_2$) mechanisms (Scheme 1).
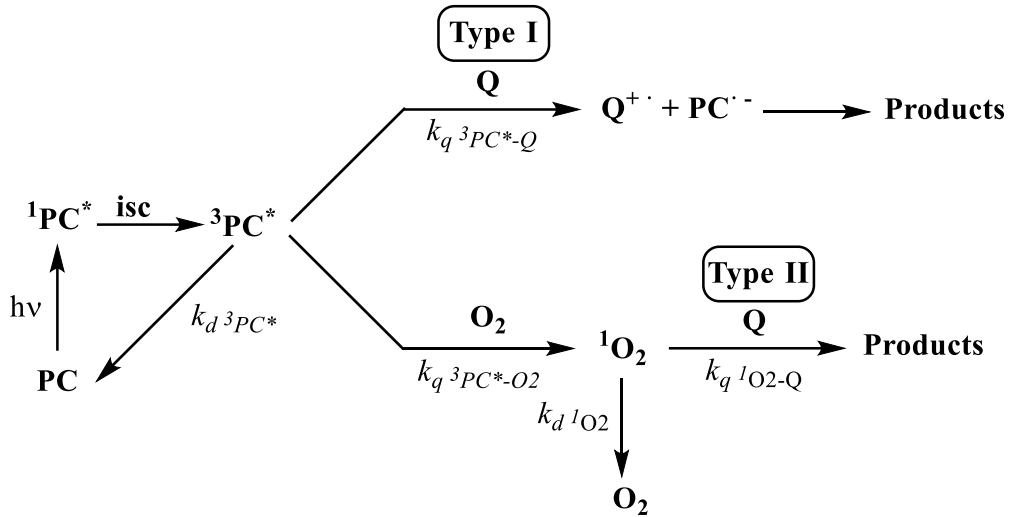
Scheme 1. Overall mechanistic pathways operating in the degradation of the pollutants photocatalyzed by the studied photocatalysts (PC = RB or PN; Q = DCF or ACP).

In fact, the triplet excited states of both photocatalysts are quenched by the pollutants (k_q *ca.* 10^7 -10^8 M^{-1}s^{-1}); but they are also quenched by O_2 (k_q *ca* 10^9 M^{-1}s^{-1}), and the resulting $^1O_2$ is subsequently quenched by the pollutants (k_q *ca.* 10^6 - 10^7 M^{-1}s^{-1}). However, to estimate the contribution of each pathway, we have to consider these data and the triplet lifetime of the photocatalysts (2.4 and 7.0 µs, for RB and PN, respectively).[22] The contribution of the three different pathways happening from the $^3PC^*$ can be calculated from equations (eq (1)-(3)):

$$\% \, Intrinsic \, triplet \, decay \, (k_{d \, ^3PC^*}) = \frac{\dfrac{1}{\tau_{^3PC^*}}}{k_{q \, ^3PC^*-O_2} \cdot [O_2] + k_{q \, ^3PC^*-Q} \cdot [Q] + \dfrac{1}{\tau_{^3PC^*}}} x100 \quad (eq \, 1)$$

Type I:

$$\% \, Quenching \, of \, the \, triplet \, by \, Q \, \left(k_{q \, ^3PC^*-Q}\right) = \frac{k_{q \, ^3PC^*-Q} \cdot [Q]}{k_{q \, ^3PC^*-O_2} \cdot [O_2] + k_{q \, ^3PC^*-Q} \cdot [Q] + \dfrac{1}{\tau_{^3PC^*}}} x100 \quad (eq \, 2)$$

$$\% \, ^1O_2 \, Formation (k_{q \, ^3PC^*-O_2}) = \frac{k_{q \, ^3PC^*-O_2} \cdot [O_2]}{k_{q \, ^3PC^*-O_2} \cdot [O_2] + k_{q \, ^3PC^*-Q} \cdot [Q] + \dfrac{1}{\tau_{^3PC^*}}} x100 \quad (eq \, 3)$$

One can consider the extreme situation, in which the quenching of $^3PC^*$ by O_2 only results in $^1O_2$ formation (eq 3); then, $^1O_2$ would evolve through two further pathways, the percentage of each one would be given by equations (4) and (5):

% $^1O_2$ Intrinsic decay $(k_{d\ ^1O_2})$

$$= \frac{k_{q\ ^3PC^*-O_2} \cdot [O_2]}{k_{q\ ^3PC^*-O_2} \cdot [O_2] + k_{q\ ^3PC^*-Q} \cdot [Q] + \frac{1}{\tau_{3PC}}} x \frac{\frac{1}{\tau\ ^1O_2}}{k\ _{^1O_2\ Q} \cdot [Q] + \frac{1}{\tau\ ^1O_2}} x100 \quad (eq\ 4)$$

Type II:

% Quenching of $^1O_2$ by Q $\left(k_{q\ ^1O_2-Q}\right)$

$$= \frac{k_{q\ ^3PC^*-O_2} \cdot [O_2]}{k_{q\ ^3PC^*-O_2} \cdot [O_2] + k_{q\ ^3PC^*-Q} \cdot [Q] + \frac{1}{\tau_{3PC^*}}} x \frac{k_{q\ ^1O_2-Q} \cdot [Q]}{k_{q\ ^1O_2-Q} \cdot [Q] + \frac{1}{\tau\ ^1O_2}} x100 \quad (eq\ 5)$$

The contribution of Type I (electron transfer to the triplet excited state of the photocatalysts) *versus* Type II (reaction with $^1O_2$) in the photodegradation of the pollutants by RB and PN has been evaluated at 10^{-5} M, an upper limit for the typical concentration of emerging pollutants in water,[23] and the results are shown on Table 2.

On one hand, when the photodegradation is performed under air, like it happens in water remediation, a competition between oxygen and the pollutants for the triplets ($^3RB^*$ or $^3PN^*$) is observed. Attending to the experimentally determined rate constants (Table 1) and the standard concentrations ($[O_2]= 2.9$ x 10^{-4} M in aqueous aerobic media),[21] formation of $^1O_2$ accounts in both cases for the major quenching pathway (> 97% for RB and >77% for PN). However, further quenching of $^1O_2$ by the pollutants is in the range of $10^6 - 10^7$ $M^{-1}s^{-1}$ (Table 1), thus at the typical contaminant concentration almost all the $^1O_2$ formed decays without

reacting. Nevertheless quenching of the triplets by the pollutants, despite its low efficiency (< 4% of triplet quenching), is the main responsible for the photodegradation.

Table 2. Estimated relative pathways reactivity in the photodegradation of DCF and ACP as shown in Scheme 1.

PC	Q	[Q] (M)	$^3PC^*$ intrinsic decay (%) eq 1	Quenching of $^3PC^*$ by Q (%) eq. 2 **Type I**	Quenching of $^3PC^*$ by O_2 (%) eq. 3	$^1O_2$ intrinsic decay (%) eq. 4	Quenching of $^1O_2$ by Q (%) eq. 5 **Type II**
RB	DCF	10^{-5}	1.5	**0.3**	98.2	98.1	**0.1**
	ACP		1.5	**0.8**	97.7	97.5	**0.2**
PN	DCF	10^{-5}	18.7	**1.5**	79.8	79.7	**0.1**
	ACP		18.3	**3.7**	77.9	77.7	**0.2**

Conclusions

The major contribution of Type I over the very often assumed Type II photodegradation mechanism, when RB is used as a photocatalyst for water remediation, has been demonstrated. The obtained fast kinetic data support this statement that is also true for PN perinaphthenone, a less commonly used photocatalyst, but with a higher singlet oxygen quantum yield formation. Therefore, photocatalysts capable of forming singlet oxygen even with a low oxidation potential are in general acting as efficient Type I oxidants from their excited states, contributing eventually this pathway more than Type II in the photodegradation. These results highlight the importance of performing a careful mechanistic study to clarify the role of each potential pathway when more than one is, in principle, possible. As exemplified herein, when photocatalysts such as RB are used as selective producers of singlet oxygen to study the

photochemistry of natural waters, their reactivity through Type I mechanism has also to be taken into account.

Acknowledgements

References

[1] Y. Usui, H. Koike, Y. Kurimura, An efficient regeneration of singlet oxygen from 2,5-diphenylfuran endoperoxide produced by a dye- sensitized oxygenation, Bull. Chem. Soc. Jpn., 60 (1987) 3373-3378.

[2] F. Wilkinson, W.P. Helman, A.B. Ross, Rate constants for the decay and reactions of the lowest electronically excited singlet-state of molecular-oxygen in solution - an expanden and revised compilation, J. Phys. Chem. Ref. Data, 24 (1995) 663-1021.

[3] M.L. Marin, L. Santos-Juanes, A. Arques, A.M. Amat, M.A. Miranda, Organic photocatalysts for the oxidation of pollutants and model compounds, Chem. Rev., 112 (2012) 1710-1750.

[4] N.A. García, F. Amat-Guerri, Photodegradation of hydroxylated N-heteroaromatic derivatives in natural-like aquatic environments: A review of kinetic data of pesticide model compounds, Chemosphere, 59 (2005) 1067-1082.

[5] D.C. Neckers, Rose Bengal, J. Photochem. Photobiol., A, 47 (1989) 1-29.

[6] Y.I. Skurlatov, L.S. Ernestova, E.V. Vichutinskaya, D.P. Samsonov, I.V. Semenova, I.Y. Rod'ko, V.O. Shvidky, R.I. Pervunina, T.J. Kemp, Photochemical transformation of polychlorinated phenols, Journal of Photochemistry and Photobiology A: Chemistry, 107 (1997) 207-213.

[7] F. Cermola, M. DellaGreca, M.R. Iesce, S. Montella, A. Pollio, F. Temussi, A mild photochemical approach to the degradation of phenols from olive oil mill wastewater, Chemosphere, 55 (2004) 1035-1041.

[8] D. Gryglik, J.S. Miller, S. Ledakowicz, Singlet molecular oxygen application for 2-chlorophenol removal, J. Hazard. Mater., 146 (2007) 502-507.

[9] J.S. Miller, Rose bengal-sensitized photooxidation of 2-chlorophenol in water using solar simulated light, Water Research, 39 (2005) 412-422.

[10] C. Lambert, T. Sarna, T.G. Truscott, Rose bengal radicals and their reactivity, J. Chem. Soc., Faraday Trans., 86 (1990) 3879-3882.

[11] C.R. Lambert, I.E. Kochevar, Electron Transfer Quenching of the Rose Bengal Triplet State, Photochem. Photobiol., 66 (1997) 15-25.

[12] N.A. Romero, D.A. Nicewicz, Organic Photoredox Catalysis, Chem. Rev., 116 (2016) 10075-10166.

[13] P.B. Merkel, D.R. Kearns, Radiationless decay of singlet molecular oxygen in solution. Experimental and theoretical study of electronic-to-vibrational energy transfer, J. Am. Chem. Soc., 94 (1972) 7244-7253.

[14] J.R. Hurst, J.D. McDonald, G.B. Schuster, Lifetime of singlet oxygen in solution directly determined by laser spectroscopy, J. Am. Chem. Soc., 104 (1982) 2065-2067.

[15] R. Martinez-Haya, J. Gomis, A. Arques, M.L. Marin, A.M. Amat, M.A. Miranda, Time-resolved kinetic assessment of the role of singlet and triplet excited states in the photocatalytic treatment of pollutants at different concentrations, Appl. Catal. B, 203 (2017) 381-388.

[16] R. Schmidt, C. Tanielian, R. Dunsbach, C. Wolff, Phenalenone, a universal reference compound for the determination of quantum yields of singlet oxygen O2(1Δg) sensitization, J. Photochem. Photobiol., A, 79 (1994) 11-17.

[17] C. Lorente, E. Arzoumanian, C. Castano, E. Oliveros, A.H. Thomas, A non-singlet oxygen mediated reaction photoinduced by phenalenone, a universal reference for singlet oxygen sensitization, RSC Advances, 4 (2014) 10718-10727.

[18] L.E. Manring, J. Eriksen, C.S. Foote, Electron-transfer photooxygenation. 4. Photooxygenation of trans-stilbene sensitized by methylene blue, J. Am. Chem. Soc., 102 (1980) 4275-4277.

[19] S.E. Braslavsky, A.U. Acuna, W. Adam, F. Amat, D. Armesto, T.D.Z. Atvars, A. Bard, E. Bill, L.O. Bjoern, C. Bohne, J. Bolton, R. Bonneau, H. Bouas-Laurent, A.M. Braun, R. Dale, K. Dill, D. Doepp, H. Duerr, M.A. Fox, T. Gandolfi, Z.R. Grabowski, A. Griesbeck, A. Kutateladze, M. Litter, J. Lorimer, J. Mattay, J. Michl, R.J.D. Miller, L. Moggi, S. Monti, S. Nonell, P. Ogilby, G. Olbrich, E. Oliveros, M. Olivucci, G. Orellana, V. Prokorenko, K.R. Naqvi, W. Rettig, A. Rizzi, R.A. Rossi, R.E. San, F. Scandola, S. Schneider, E.W. Thulstrup, B. Valeur, J. Verhoeven, J. Warman, R. Weiss, J. Wirz, K. Zachariasse, Glossary of Terms Used in Photochemistry, 3rd edition (IUPAC recommendations 2006), Pure Appl. Chem., 79 (2007) 293-465.

[20] D. Rehm, A. Weller, Kinetics of fluorescence quenching by electron and H-atom transfer, Isr. J. Chem., 8 (1970) 259-271.

[21] S.L. Murov, I. Carmichael, G.L. Hug, Handbook of Photochemistry, 2nd ed., Marcel Dekker, New York, 2009.

[22] A. Penzkofer, M. Simmel, D. Riedl, Room temperature phosphorescence lifetime and quantum yield of erythrosine B and rose bengal in aerobic alkaline aqueous solution, J. Lumin., 132 (2012) 1055-1062.

[23] D. Fatta-Kassinos, S. Meric, A. Nikolaou, Pharmaceutical residues in environmental waters and wastewater: current state of knowledge and future research, Analytical and Bioanalytical Chemistry, 399 (2011) 251-275.